Int. J. Solids Structures Vol. 23, No. 1, pp. 175–185, 1987
Printed in Great Britain.

0020-7683/87 $3.00 + .00
Pergamon Journals Ltd.

OUT-OF-PLANE VIBRATIONS OF THICK RINGS

C. S. TANG and C. W. BERT
School of Aerospace, Mechanical and Nuclear Engineering, The University of Oklahoma, Norman, OK 73019, U.S.A.

(*Received* 4 *October* 1985; *in revised form January* 1986)

Abstract—Depending on its cross-sectional geometry, a ring can be modelled by at least three different theories. Kirkhope developed a simple ring theory which is applicable to out-of-plane vibrations of rings with small cross-sectional aspect ratio (i.e. compact rings and shell-like rings). For plate-like rings, the present analysis uses a Levinson-type plate theory to analyze the out-of-plane vibrations. Also, a three-dimensional finite-element analysis using NASTRAN shows better agreement than results of Kirkhope's ring theory and Mindlin's thick plate theory.

NOTATION

$A_1, \ldots, A_6$	coefficients in the general solution of w_1, w_2, w_3
a	outer radius
b	radial thickness
D	out-of-plane bending stiffness $= Eh^3/[12(1-\nu^2)]$
E, G	elastic and shear moduli
$F_1, \ldots, F_4$	functions defined in eqns (37) and (38)
f, g	parameters defined in eqns (30)
h	axial thickness
I	mass moment of inertia about midplane $= \rho h^3/12$
I_n, K_n	modified Bessel functions of the first and second kind
J_n, Y_n	Bessel functions of the first and second kind
M	bending and twisting stress couples
n	circumferential wave number
Q	plane-stress reduced stiffness $= E/(1-\nu^2)$
Q_x, Q_y	transverse shear stress resultants
r	radius of ring cross section
R	centroidal radius of ring cross section
t	time
U, V, W	generalized displacements
$\bar{u}, \bar{v}, \bar{w}$	displacement parameters introduced in eqns (42)–(44)
w	z-direction displacement
w_1, w_2, w_3	uncoupling displacement potentials
$\bar{w}_1, \bar{w}_2, \bar{w}_3$	dimensionless versions of w_1, w_2, w_3, normalized by radius a
x, y, z	Cartesian coordinates
$\nabla^2, \bar{\nabla}^2$	Laplacian operators with respect to dimensional and dimensionless coordinates (normalized by radius a)
γ, ε	shear and normal strains
η	nondimensionalized radius (r/a)
θ	angular dimensional variable
$\lambda_1, \lambda_2, \lambda_3$	uncoupled dimensionless eigenfrequencies; see eqns (33)
ν	Poisson's ratio
ξ	indicator functions defined in eqns (37) and (38)
σ, τ	normal and shear stresses
Φ_x, Φ_y	higher-order displacement parameters
ψ_x, ψ_y	bending slopes
Ω	nondimensionalized frequency, $\omega h\sqrt{(\rho/G)}$
ω	eigenfrequency.

1. INTRODUCTION

Rings have long been widely used as structural elements and hence have attracted engineering interest. For rings with material and geometric symmetry with respect to the centroidal plane, the in-plane and out-of-plane modes are uncoupled. The in-plane modes of thick rings were analyzed most recently by Gardner and Bert[1] who generalized the approach of Levinson's straight beam theory[2]. For out-of-plane modes, the present research provides an analytical solution using the dynamic version of Levinson's plate theory[3] and a three-dimensional finite-element solution.

The classical theory for out-of-plane motion of thin rings can be traced back to the work of Michell[4] in 1890 and Love[5] in 1899. The improved theories taking into account transverse shear deformation and rotatory inertia were pioneered even earlier by Bresse[6] in 1859, and followed by Timoshenko[7, 8] in 1921–22. Other notable studies include the contributions of Hammond and Archer[9] and Rao[10]. Experimental studies have also been carried out by Peterson[11] and by Kuhl[12]. Recently, Kirkhope developed a very simple yet accurate theory[13].

A similar hierarchy exists in the plate theories. Various theories were introduced to remedy the deficiencies of the classical thin plate theory due to Germaine and Lagrange. Reissner[14, 15] and Mindlin[16] made notable attempts to include transverse shear deformation. A more realistic transverse shear strain distribution was obtained in the theories of Ambartsumyan[17], Reissner[18, 19] and Levinson[3]. In the present paper, a Levinson-type plate theory is derived to analyze the out-of-plane dynamics of thick rings.

With careful modelling practices, the state-of-the-art finite-element methods can be used as an engineering tool for numerical modal experiments. For very thin rings, curved beam elements in the work of Sabir and Ashwell[20] and Davis *et al.*[21] can be employed. Notable plate and shell elements were developed by Anderson *et al.*[22] and Clough and Wilson[23], respectively. However, to analyze the relatively thick rings, a three-dimensional continuum model is preferred, since it is easy to use and inherits no deficiency from the engineering theories mentioned above.

Depending upon the cross-sectional aspect ratio, rings can have the attributes of curved beams, thick annular plates, or short cylindrical shells. They can be analyzed with different engineering theories accordingly. Kirkhope's work[13] is appropriate for compact and shell-like rings. Yet for rings of medium aspect ratio such as considered in Ref. [1], the Levinson-type plate theory shows better agreement with a rigorous finite-element analysis using NASTRAN[24] which further agrees both accurately and consistently with experimental results for the in-plane modes and some other cases considered by Kirkhope[13].

2. ANALYSIS USING LEVINSON-TYPE PLATE THEORY

All three of the displacements have to be considered due to twisting which does not appear in in-plane analysis. Strains and stresses are obtained and then integrated through the thickness to yield the stress resultants. Applying force equilibrium on an infinitesimal element gives the governing differential equations which can be uncoupled by defining three potential functions appropriately. Finally, the frequency equation is obtained by applying free–free boundary conditions.

The circular ring considered has a rectangular cross section and is free on all boundaries. Other assumptions are as follows:

1. The material is homogeneous, linearly elastic, and isotropic.
2. The strain–displacement relations are linear (i.e. displacements are small).
3. Transverse normal strain is negligible.
4. No body forces are present.

To impose a parabolic distribution of transverse shear strain, the in-plane displacements can be assumed to be cubic. Using Hypothesis 3, the three rectangular-coordinate displacements are approximated by:

$$U(x,y,z,t) = z\Psi_x(x,y,t) - \frac{4z^3}{3h^2}\Phi_x(x,y,t) \tag{1}$$

$$V(x,y,z,t) = z\Psi_y(x,y,t) - \frac{4z^3}{3h^2}\Phi_y(x,y,t) \tag{2}$$

$$W(x,y,z,t) = w(x,y,t). \tag{3}$$

The transverse shear strain components vanish at the upper and lower surfaces:

$$\gamma_{yz} = V_{,z} + W_{,y} = \Psi_y - \frac{4z^2}{h^2}\Phi_y + w_{,y} = 0 \qquad \text{at } z = \pm\frac{h}{2}.$$

Thus,

$$\Phi_y = \Psi_y + w_{,y}. \tag{4}$$

Similarly,

$$\Phi_x = \Psi_x + w_{,x}. \tag{5}$$

Accordingly, the strains can be derived as:

$$\varepsilon_x = U_{,x} = z\Psi_{x,x} - \frac{4z^3}{3h^2}(\Psi_{x,x} + w_{,xx}) \tag{6}$$

$$\varepsilon_y = V_{,y} = z\Psi_{y,y} - \frac{4z^3}{3h^2}(\Psi_{y,y} + w_{,yy}) \tag{7}$$

$$\varepsilon_z = 0 \tag{8}$$

$$\gamma_{yz} = V_{,z} + W_{,y} = \left(1 - \frac{4z^2}{h^2}\right)(\Psi_y + w_{,y}) \tag{9}$$

$$\gamma_{zx} = U_{,z} + W_{,x} = \left(1 - \frac{4z^2}{h^2}\right)(\Psi_x + w_{,x}) \tag{10}$$

$$\gamma_{xy} = U_{,y} + V_{,x} = z(\Psi_{x,y} + \Psi_{y,x}) - \frac{4z^3}{3h^2}(\Psi_{x,y} + \Psi_{y,x} + 2w_{,xy}). \tag{11}$$

Generalized Hooke's law together with the condition $\sigma_z = 0$ requires that:

$$\begin{Bmatrix}\sigma_x\\ \sigma_y\\ \tau_{xy}\end{Bmatrix} = Q\begin{bmatrix}1 & \nu & 0\\ \nu & 1 & 0\\ 0 & 0 & \dfrac{1-\nu}{2}\end{bmatrix}\left[z\begin{Bmatrix}\Psi_{x,x}\\ \Psi_{y,y}\\ \Psi_{x,y}+\Psi_{y,x}\end{Bmatrix} - \frac{4z^3}{3h^2}\begin{Bmatrix}\Psi_{x,x}+w_{,xx}\\ \Psi_{y,y}+w_{,yy}\\ \Psi_{x,y}+\Psi_{y,x}+2w_{,xy}\end{Bmatrix}\right] \tag{12}$$

$$\begin{Bmatrix}\tau_{xz}\\ \tau_{yz}\end{Bmatrix} = G\left(1 - \frac{4z^2}{h^2}\right)\begin{Bmatrix}\Psi_x + w_{,x}\\ \Psi_y + w_{,y}\end{Bmatrix}. \tag{13}$$

The generalized forces are defined as:

$$\begin{Bmatrix}M_x\\ M_y\\ M_{xy}\end{Bmatrix} = \int_{-h/2}^{h/2} z\begin{Bmatrix}\sigma_x\\ \sigma_y\\ \tau_{xy}\end{Bmatrix}\mathrm{d}z = D\begin{bmatrix}1 & \nu & 0\\ \nu & 1 & 0\\ 0 & 0 & \dfrac{1-\nu}{2}\end{bmatrix}\left[\begin{Bmatrix}\Psi_{x,x}\\ \Psi_{y,y}\\ \Psi_{x,y}+\Psi_{y,x}\end{Bmatrix} - \frac{1}{5}\begin{Bmatrix}\Psi_{x,x}+w_{,xx}\\ \Psi_{y,y}+w_{,yy}\\ \Psi_{x,y}+\Psi_{y,x}+2w_{,xy}\end{Bmatrix}\right] \tag{14}$$

$$\begin{Bmatrix}Q_x\\ Q_y\end{Bmatrix} = \int_{-h/2}^{h/2}\begin{Bmatrix}\tau_{xz}\\ \tau_{yz}\end{Bmatrix}\mathrm{d}z = \frac{2Gh}{3}\begin{Bmatrix}\Psi_x + w_{,x}\\ \Psi_y + w_{,y}\end{Bmatrix}. \tag{15}$$

Integrating the left-hand sides of the stress equilibrium equations gives the generalized force equilibrium equations as follows:

$$\int_{-h/2}^{h/2} z(\sigma_{x,x}+\tau_{xy,y}+\tau_{xz,z}-\rho U_{,tt})\,dz = 0 \tag{16}$$

$$\int_{-h/2}^{h/2} z(\tau_{xy,x}+\sigma_{y,y}+\tau_{yz,z}-\rho V_{,tt})\,dz = 0 \tag{17}$$

$$\int_{-h/2}^{h/2} (\tau_{xz,x}+\tau_{yz,y}+\sigma_{z,z}-\rho W_{,tt})\,dz = 0. \tag{18}$$

Then

$$M_{x,x}+M_{xy,y}-Q_x = \frac{5}{4}I\Psi_{x,tt}-\frac{5}{16}Iw_{,xtt} \tag{19}$$

$$M_{xy,x}+M_{y,y}-Q_y = \frac{5}{4}I\Psi_{y,tt}-\frac{5}{16}Iw_{,ytt} \tag{20}$$

$$Q_{x,x}+Q_{y,y} = \rho h w_{,tt}. \tag{21}$$

Substituting eqns (14), (15) in eqns (19), (20), (21) yields the governing differential equations in terms of the generalized displacements:

$$D\left(\Psi_{x,xx}+\frac{1-\nu}{2}\Psi_{x,yy}+\frac{1+\nu}{2}\Psi_{y,xy}-\underline{\tfrac{1}{4}\nabla^2 w_{,x}}\right)-\frac{5Gh}{6}(\Psi_x+w_{,x}) = I\Psi_{x,tt}-\underline{\tfrac{1}{4}Iw_{,xtt}} \tag{22}$$

$$D\left(\frac{1+\nu}{2}\Psi_{x,xy}+\frac{1-\nu}{2}\Psi_{y,xx}+\Psi_{y,yy}-\underline{\tfrac{1}{4}\nabla^2 w_{,y}}\right)-\frac{5Gh}{6}(\Psi_y+w_{,y}) = I\Psi_{y,tt}-\underline{\tfrac{1}{4}Iw_{,ytt}} \tag{23}$$

$$\underline{\underline{\frac{2G}{3}}}(\Psi_{x,x}+\Psi_{y,y}+\nabla^2 w) = \rho w_{,tt}. \tag{24}$$

It is noted that the differences between the above equations and Reissner–Mindlin theory are the presence of the underlined terms and the doubly underlined $2G/3$ instead of $5G/6$.

To uncouple eqns (22), (23), (24), three potential functions similar to those in [16] are defined as follows:

$$\Psi_x = [(f-1)w_{1,x}+(g-1)w_{2,x}+w_{3,y}]\cos\omega t \tag{25}$$

$$\Psi_y = [(f-1)w_{1,y}+(g-1)w_{2,y}-w_{3,x}]\cos\omega t \tag{26}$$

$$w = (w_1+w_2)\cos\omega\tau. \tag{27}$$

Substituting the above equations in eqns (22), (23), (24) gives

$$D(f-1.25)\left[\nabla^2 w_1+\left(\frac{I\omega^2}{D}-\frac{5Ghf}{6(f-1.25)D}\right)w_1\right]_{,x}$$
$$+D(g-1.25)\left[\nabla^2 w_2+\left(\frac{I\omega^2}{D}-\frac{5Ghg}{6(g-1.25)D}\right)w_2\right]_{,x}$$
$$+\frac{1-\nu}{2}D\left[\nabla^2 w_3+\frac{2}{1-\nu}\left(\frac{I\omega^2}{D}-\frac{5Gh}{6D}\right)w_3\right]_{,y}=0 \quad (28)$$

and

$$f\left(\nabla^2 w_1+\frac{3\rho\omega^2}{2Gf}w_1\right)+g\left(\nabla^2 w_2+\frac{3\rho\omega^2}{2Gg}w_2\right)=0. \quad (29)$$

To make eqns (28), (29) consistent, f and g are defined as:

$$\begin{Bmatrix} f \\ g \end{Bmatrix}=\frac{(17-5\nu)\pm\sqrt{\left((7+5\nu)^2+\dfrac{2400(1-\nu)}{\Omega^2}\right)}}{8(1-\nu)\left(1-\dfrac{10}{\Omega^2}\right)}. \quad (30)$$

Then the three uncoupled equations of motion are

$$(\bar{\nabla}^2+\xi\zeta_i^2)\bar{w}_i=0 \qquad (i=1,3) \quad (31)$$

$$(\bar{\nabla}^2+\lambda_2^2)\bar{w}_2=0 \quad (32)$$

where λ_1, λ_2, and λ_3 can be seen as the dimensionless natural frequencies of the three uncoupled displacements (w_1, w_2 and w_3) and can be expressed in terms of the dimensionless frequency Ω as

$$\lambda_1\equiv[\sqrt{(6\xi/5f)}](a/h)\Omega, \quad \lambda_2\equiv[\sqrt{(6/5g)}](a/h)\Omega, \quad \lambda_3\equiv[\sqrt{((\Omega^2-10)\xi)}](a/h). \quad (33)$$

For circular rings, appropriate solutions can be expressed in terms of Bessel functions as follows:

$$\bar{w}_1=[A_1F_1(\lambda_1\eta)+A_2F_2(\lambda_1\eta)]\cos n\theta \quad (34)$$

$$\bar{w}_2=[A_3F_3(\lambda_2\eta)+A_4F_4(\lambda_2\eta)]\cos n\theta \quad (35)$$

$$\bar{w}_3=[A_5F_1(\lambda_3\eta)+A_6F_2(\lambda_3\eta)]\sin n\theta \quad (36)$$

where

$$\text{if } \Omega^2<10, \quad \xi=-1, \quad F_1=I_n, \quad F_2=K_n, \quad F_3=J_n, \quad F_4=Y_n \quad (37)$$

$$\text{if } \Omega^2>10, \quad \xi=1, \quad F_1=J_n, \quad F_2=Y_n, \quad F_3=J_n, \quad F_4=Y_n. \quad (38)$$

For thick plates, the appropriate free–free boundary conditions are $Q_r=M_r=M_{r\theta}=0$. To simplify the algebra, take $\theta=0°$. So $Q_x=M_{xy}=M_x=0$ at ($x=a,b$, $y=0$ or

$\eta = b/a, 1$). Then, the resulting six equations comprise an eigenvalue problem as follows:

$$A_1[f\lambda_1 F_1'(\lambda_1\eta)]+A_2[f\lambda_1 F_2'(\lambda_1\eta)]+A_3[g\lambda_2 F_3'(\lambda_2\eta)]+A_4[g\lambda_2 F_4'(\lambda_2\eta)] + A_5\left[\frac{n}{\eta}F_1(\lambda_3\eta)\right]+A_6\left[\frac{n}{\eta}F_2(\lambda_3\eta)\right]=0 \quad (39)$$

$$A_1\left[(2f-2.5)\frac{n\lambda_1}{\eta}F_1'(\lambda_1\eta)\right]+A_2\left[(2f-2.5)\frac{n\lambda_1}{\eta}F_2'(\lambda_2\eta)\right] + A_3\left[(2g-2.5)\frac{n\lambda_2}{\eta}F_3'(\lambda_2\eta)\right]+A_4\left[(2g-2.5)\frac{n\lambda_2}{\eta}F_4'(\lambda_2\eta)\right] + A_5\left[\lambda_3^2F_1''(\lambda_3\eta)+\frac{n^2}{\eta^2}F_1(\lambda_3\eta)\right]+A_6\left[\lambda_3^2F_2''(\lambda_3\eta)+\frac{n^2}{\eta^2}F_2(\lambda_3\eta)\right]=0 \quad (40)$$

$$A_1(f-1.25)\left[\lambda_1^2F_1''(\lambda_2\eta)-\frac{\nu n^2}{\eta^2}F_1(\lambda_1\eta)\right]+A_2(f-1.25)\left[\lambda_1^2F_2''(\lambda_1\eta)-\frac{\nu n^2}{\eta^2}F_2(\lambda_1\eta)\right] + A_3(g-1.25)\left[\lambda_2^2F_3''(\lambda_2\eta)-\frac{\nu n^2}{\eta^2}F_3(\lambda_2\eta)\right]+A_4(g-1.25)\left[\lambda_2^2F_4''(\lambda_2\eta)-\frac{\nu n^2}{\eta^2}F_4(\lambda_2\eta)\right] + A_5(1-\nu)\left[\frac{\lambda_3 n}{\eta}F_1'(\lambda_3\eta)\right]+A_6(1-\nu)\left[\frac{\lambda_3 n}{\eta}F_2'(\lambda_3\eta)\right]=0. \quad (41)$$

The corresponding 6×6 matrix does not take any of the standard forms and hence cannot be solved by matrix methods. Also, the expanded determinant is both implicit and complicated algebraically in terms of Ω^2, a characteristic that calls for a direct equation solving algorithm such as binary division, etc. The FORTRAN program developed first calculates the coefficients in which the values of the Bessel functions and their derivatives are calculated by some IMSL subroutines[26] and recursive formulas[27]. Then Gauss elimination is employed to obtain the determinant which in turn is taken as the dependent function value in the equation solving subroutine.

3. ANALYSIS USING THE FINITE-ELEMENT METHOD

The physical ring analyzed here is compact as shown in Fig. 1. To model it, a twenty-node isoparametric solid element HEXA[24], has been chosen in MSC/NASTRAN. The

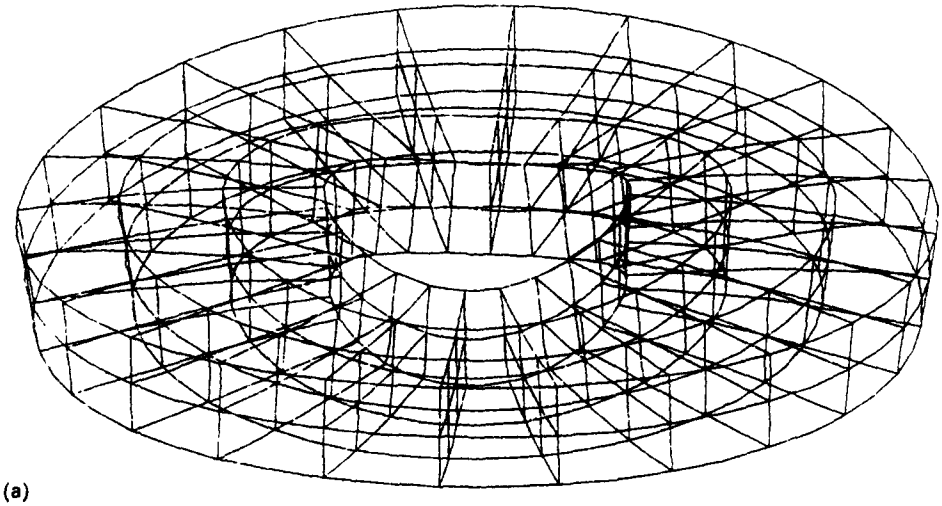

(a)

Fig. 1. Out of plane mode shapes: (a) mode 2, (b) mode 3, (c) mode 4, (d) mode 5.

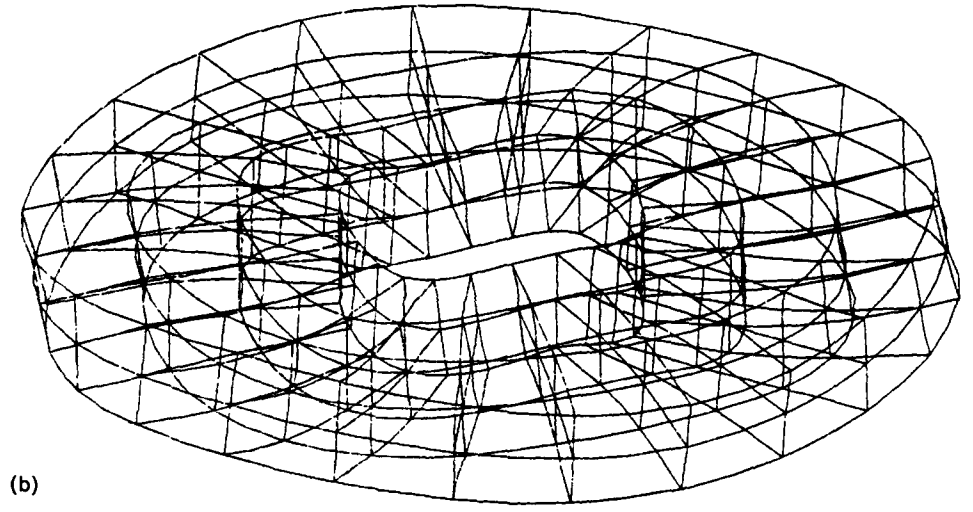

(b)

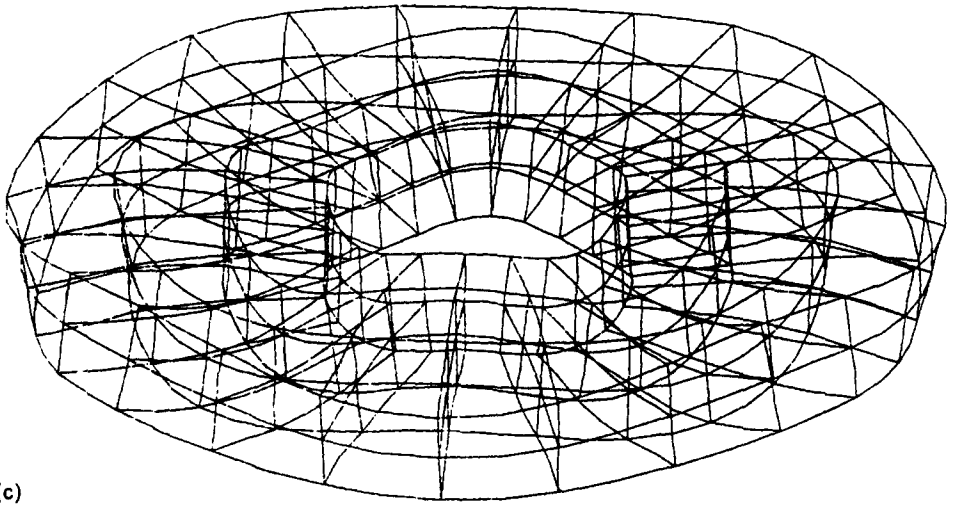

(c)

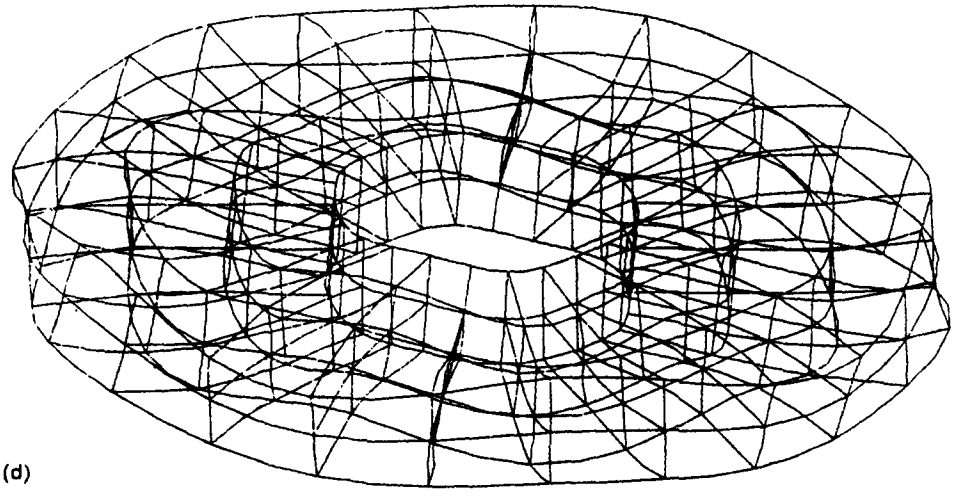

(d)

Fig. 1—*continued*

outputs from a FORTRAN preprocessor are merged to other card decks to formulate input to NASTRAN. The in-plane and out-of-plane modes can be identified easily with the aid of the plotted mode shapes.

A FORTRAN program is used to generate all the nodes, connectivity and multiple constraint conditions.

Each node has three translational degrees of freedom. The model shown has $41 \times 24 = 984$ nodes and hence $984 \times 3 = 2952$ degrees of freedom.

Since the three displacements can be expressed as:

$$U(r, \theta, z, t) = \bar{u}(r, z) \cos n\theta \cos \omega t \tag{42}$$

$$V(r, \theta, z, t) = \bar{v}(r, z) \sin n\theta \cos \omega t \tag{43}$$

$$W(r, \theta, z, t) = \bar{w}(r, z) \cos n\theta \cos \omega t \tag{44}$$

the three-dimensional model can be fully specified by a two-dimensional fictitious field which has been chosen arbitrarily as the cross section of $\theta = 0°$. In this planar region there are 20 nodes, so the number of degrees of freedom is reduced to $29 \times 3 = 87$ which is only 2.95% of that of the original model. This reduction is incorporated by the MPC (multiple point constraint) cards generated by the FORTRAN preprocessor mentioned above.

4. NUMERICAL RESULTS AND DISCUSSION

The geometric parameters of a thick ring with rectangular cross section are b/R and the aspect ratio b/h. The accuracy of different methods for different rings is illustrated with several examples. See Tables 1 and 2 for material properties and physical dimensions, respectively.

First, consider two steel rings both with $b/h = 1$ but having $b/R = 0.479$ and 0.75, respectively. The experimental, classical thin-ring theory, and Kirkhope-theory data are taken from [13]. Classical solution gives errors well exceeding 100% while the Kirkhope-theory errors are remarkably small, as shown in Tables 3 and 4. The Levinson-type thick-plate theory errs least at mode three but is not applicable for this small an aspect ratio. The percentage error of the finite-element result is medium but consistent both in sign and magnitude.

The second case considered is a series of rings with the same outer radius $a = 9.375$ in. and radial thickness $b = 1.063$ in. Also, they can be considered thin radially ($b/R = 0.113$). The axial thickness varies from 0.625 to 3.5 in. ($b/h = 1.7$–0.3). Kirkhope's

Table 1. Material properties used in subsequent calculations

Material	Elastic modulus, psi	Poisson's ratio	Density lb-sec^2/in.^{4}	Tables in which used
Steel	30.0×10^6	0.29	7.33×10^{-4}	2–4
Aluminum	10.1×10^6	0.333	2.59×10^{-4}	5

Table 2. Physical dimensions of rings considered in subsequent tables

	Table 3	4	5	6, 7
Outer radius, a (mm)	1.772(45.00)	1.772(45.00)	*	4.50(114.3)
Radial thickness, b (mm)	0.685(17.13)	0.967(24.6)	*	1.50 (38.1)
Axial thickness, h (mm)	0.685(17.13)	0.967(24.6)	*	1.00 (25.4)

* Numerous values are used in Table 5, and they are presented in that table.

Table 3. Natural frequencies corresponding to out-of-plane modes of rectangular-cross-section steel ring ($b/h = 1$, $b/R = 0.479$)

Mode No. (n)	Experimental, Kuhl[12] (Hz)	Classical thin (% error)	Kirkhope (% error)	Levinson plate (% error)	FEM (NASTRAN) (% error)
2	2605	212	0.00	23.0	−1.9
3	7330	218	0.04	15.8	−4.4
4	13,750	227	0.25	3.5	−1.6
5	21,450	240	0.46	−8.0	−2.2

Table 4. Natural frequencies corresponding to out-of-plane modes of rectangular-cross-section steel ring ($b/h = 1$, $b/R = 0.75$)

Mode No. (n)	Experimental, Kuhl[12] (Hz)	Classical thin (% error)	Kirkhope (% error)	Levinson plate (% error)	FEM (NASTRAN) (% error)
2	6620	113	2.54	47.4	−14.3
3	16,790	141	3.80	24.0	−15.8
4	28,700	172	4.04	−4.8	−8.6
5	41,200	207	4.66	9.6	−14.1

Table 5. Natural frequencies corresponding to out-of-plane mode of rectangular-cross-section steel rings
($a = 9.375$ in., $b = 1.063$ in., $n = 2$)

h (in.)	Experimental, Peterson[11] (Hz)	Classical thin (% error)	Kirkhope (% error)	FEM (NASTRAN) (% error)
0.625	200	3.0	−1.0	−1.5
1.500	420	6.5	−0.5	−1.2
2.500	575	24.9	−1.2	−2.1
3.500	640	54.5	−0.8	−1.4

($a = 9.375$ in., $b = 8.063$ in., $n = 2$)

h (in.)	Classical thin (Hz)	Kirkhope (Hz)	Levinson plate (Hz)	FEM (NASTRAN) (Hz)
0.625	374	361	355	358
1.500	891	848	839	834
2.500	1459	1354	1328	1325
3.500	2000	1795	1756	1749

Table 6. Natural frequencies corresponding to out-of-plane modes of rectangular-cross-section aluminum ring ($b/h = 3$, $b/R = 1$)

Mode No. (n)	Classical thin (Hz)	Kirkhope simplified (Hz)	Kirkhope (Hz)	Mindlin plate* (Hz)	Levinson plate* (Hz)	FEM (NASTRAN)* (Hz)
2	13,674	12,959	12,355	11,274	10,955	11,353
3	39,217	36,248	31,357	17,363	18,868	16,423
4	75,636	68,750	53,184	22,488	22,783	21,331
5	122,676	109,447	76,181	26,949	26,678	25,970

* Calculated in the present investigation.

theory and the finite-element method show good results compared to Peterson's experimental results[11], while the classical theory accumulates large errors with large bs, as can be seen in Table 5 (top). Since the rings considered are not plate like, another series of fictitious rings with the same dimensions except that $b = 8.063$ in. ($b/R = 1.42$) are considered. Here, the results by Levinson's and Kirkhope's theories and the finite-element method are very close. Again, the classical theory gives higher predictions. See Table 5 (bottom).

The aluminum ring, the in-plane modes of which were studied in [1], is specified by $b/h = 3$ and $b/R = 1$ and is more like an annular plate. For the out-of-plane modes, the eigenfrequencies calculated with various methods are listed in Table 6. Figure 1 shows the mode shapes for modes 2 through 5. Since the ring cross section is very compact, the classical solutions are expected to be too high. Kirkhope's theories show little decrease. Also, nearly the same result as that of the classical solution is found in the table of the paper by Irie *et al.*[25], which is based on Mindlin's plate theory. Since their table covers up to the second mode only, no comparison for higher modes is available and its validity is subjected to doubt. The Levinson-type plate theory and the finite-element method give substantial reduction and match well with each other.

This problem was solved herein using Mindlin plate theory and essentially the same methodology as for the Levinson-type plate theory. These results differ from the result (for one mode only) given in [25] and are presented in Table 5.

5. CONCLUDING REMARKS

Engineers like inexpensive but reasonably accurate methods. Among the various theories mentioned above, classical theory is the easiest but yet most inaccurate one. The opposite is the elasticity theory. Combining the results, some suggestions can be made as follows:

1. For plate-like rings, Levinson-type plate theory predicts good eigenfrequencies and a more realistic strain profile.
2. For other compact rings, Kirkhope's theories are good.
3. The finite-element method can be used as a verification with good accuracy and reasonable prices (nearly ten minutes of CPU time of NASTRAN on IBM 370 for four modes).

REFERENCES

1. T. G. Gardner and C. W. Bert, Vibration of shear deformable rings: theory and experiment. *J. Sound Vib.* **103**, 549 (1985).
2. M. Levinson, A new rectangular beam theory. *J. Sound Vib.* **74**, 81 (1981).
3. M. Levinson, An accurate, simple theory of the statics and dynamics of elastic plates. *Mech. Rsch. Comm.* **7**, 343 (1980).
4. J. H. Michell, The small deformation of curves and surfaces with application to the vibrations of a helix and a circular ring. *Mess. Math.* **19**, 68 (1890).
5. A. E. H. Love, *A Treatise on the Mathematical Theory of Elasticity*, 4th edn, pp. 451–454. Dover, New York (1944).
6. J. A. C. Bresse, *Cours de Mécanique Appliquée*, 2nd edn. Gauthier-Villars, Paris (1859).
7. S. P. Timoshenko, On the correction for shear of the differential equation for transverse vibration of prismatic bars. *Phil. Mag.* Ser. 6 **41**, 744 (1921).
8. S. P. Timoshenko, On the transverse vibrations of bars of uniform cross section. *Phil. Mag.* Ser. 6 **43**, 125 (1922).
9. A. S. Hammond and R. R. Archer, On the free vibration of complete and incomplete rings. *Dev. Mech. Proc.* **2**, 489 (1963).
10. S. S. Rao, Effects of transverse shear and rotary inertia on the coupled twist-bending vibration of circular rings. *J. Sound Vib.* **16**, 551 (1971).
11. R. E. Peterson, Natural frequency of gears. *Trans. ASME* **52**, Paper APM-52-1, pp. 1–11 (1930).
12. W. Kuhl, Messungen zu den theorien der eigenschwingungen von kreisringen beliebiger wandstarke. *Akustiche Zeitschrift* **7**(7), 10 (1942).
13. J. Kirkhope, Out-of-plane vibration of thick circular ring. *J. Engng Mech. Div. ASCE* **102** (EM2), 239 (1976).
14. E. Reissner, On the theory of bending of elastic plates. *J. Math. Phys.* **23**, 184 (1944).
15. E. Reissner, The effect of transverse shear deformation on the bending of elastic plates. *J. Appl. Mech.* **12**, A69 (1945).
16. R. D. Mindlin, Influence of rotatory inertia and shear on flexural motions of isotropic, elastic plates. *J. Appl. Mech.* **18**, 31 (1951).

17. S. A. Ambartsumyan, *Theory of Anisotropic Plates* (English translation by T. Cheron, edited by J. E. Ashton). Technomic, Stamford, CT (1970).
18. E. Reissner, On transverse bending of plates, including the effect of transverse shear deformation. *Int. J. Solids Structures* **11**, 569 (1975).
19. E. Reissner and J. E. Reissner, A problem of unsymmetrical bending of shear-deformable circular ring plates. *Ingenieur-Archiv* **55**, 57 (1985).
20. A. B. Sabir and D. G. Ashwell, A comparison of curved beam finite elements when used in vibration problems. *J. Sound Vib.* **18**, 555 (1971).
21. R. Davis, R. D. Henshell and G. B. Warburton, Curved beam finite elements for coupled bending vibration. *Int. J. Earthquake Engng Struct. Dyn.* **1**, 165 (1972).
22. R. G. Anderson, B. M. Irons and O. C. Zienkiewicz, Vibration and stability of plates using finite elements. *Int. J. Solids Structures* **4**, 1031 (1968).
23. R. W. Clough and E. L. Wilson, Dynamic finite element analysis of arbitrary thin shells. *Comput. Struct.* **1**, 33 (1971).
24. *MSC/NASTRAN User's Manual*, 64. MacNeal-Schwendler Corp., Los Angeles, CA (1984).
25. Y. Irie, G. Yamada and K. Takagi, Natural frequencies of thick annular plates. *J. Appl. Mech.* **49**, 633 (1982).
26. *IMSL Library Reference Manual*, 9th edn. IMSL Inc., Houston, TX (1982).
27. G. N. Watson, *A Treatise on the Theory of Bessel Functions*, 2nd edn. Cambridge University Press, London (1944).